

**AWARD NUMBER:** W81XWH-14-1-0049

**TITLE:** Using T2-Exchange from Ln3+DOTA-Based Chelates for Contrast-Enhanced Molecular Imaging of Prostate Cancer with MRI

**PRINCIPAL INVESTIGATOR:** Todd C. Soesbe, Ph.D.

**CONTRACTING ORGANIZATION:** University of Texas Southwestern Medical Center at Dallas  
Dallas, Texas 75390-8568

**REPORT DATE:** April 2015

**TYPE OF REPORT:** Annual

**PREPARED FOR:** U.S. Army Medical Research and Materiel Command  
Fort Detrick, Maryland 21702-5012

**DISTRIBUTION STATEMENT:** Approved for Public Release;  
Distribution Unlimited

The views, opinions and/or findings contained in this report are those of the author(s) and should not be construed as an official Department of the Army position, policy or decision unless so designated by other documentation.

<b>REPORT DOCUMENTATION PAGE</b>		<i>Form Approved</i> <i>OMB No. 0704-0188</i>	
Public reporting burden for this collection of information is estimated to average 1 hour per response, including the time for reviewing instructions, searching existing data sources, gathering and maintaining the data needed, and completing and reviewing this collection of information. Send comments regarding this burden estimate or any other aspect of this collection of information, including suggestions for reducing this burden to Department of Defense, Washington Headquarters Services, Directorate for Information Operations and Reports (0704-0188), 1215 Jefferson Davis Highway, Suite 1204, Arlington, VA 22202-4302. Respondents should be aware that notwithstanding any other provision of law, no person shall be subject to any penalty for failing to comply with a collection of information if it does not display a currently valid OMB control number. <b>PLEASE DO NOT RETURN YOUR FORM TO THE ABOVE ADDRESS.</b>			
<b>1. REPORT DATE</b> April 2015		<b>2. REPORT TYPE</b> Annual	
		<b>3. DATES COVERED</b> 1 Feb 2014 - 31 Jan 2015	
<b>4. TITLE AND SUBTITLE</b>  Using T2-Exchange from Ln3+DOTA-Based Chelates for Contrast-Enhanced Molecular Imaging of Prostate Cancer with MRI		<b>5a. CONTRACT NUMBER</b>	
		<b>5b. GRANT NUMBER</b> W81XWH-14-1-0049	
		<b>5c. PROGRAM ELEMENT NUMBER</b>	
<b>6. AUTHOR(S)</b> Todd C. Soesbe, Ph.D. Yunkou Wu, Ph.D. James Ratnaker, Ph.D. Mark Milne, Ph.D. Lei Zhang A. Dean Sherry, Ph.D.   E-Mail: todd.soesbe@utsouthwestern.edu		<b>5d. PROJECT NUMBER</b>	
		<b>5e. TASK NUMBER</b>	
		<b>5f. WORK UNIT NUMBER</b>	
<b>7. PERFORMING ORGANIZATION NAME(S) AND ADDRESS(ES)</b>  UT Southwestern Medical Center at Dallas 5323 Harry Hines BLVD, Dallas, Texas, 75390-8568		<b>8. PERFORMING ORGANIZATION REPORT NUMBER</b>	
<b>9. SPONSORING / MONITORING AGENCY NAME(S) AND ADDRESS(ES)</b>  U.S. Army Medical Research and Materiel Command Fort Detrick, Maryland 21702-5012		<b>10. SPONSOR/MONITOR'S ACRONYM(S)</b>	
		<b>11. SPONSOR/MONITOR'S REPORT NUMBER(S)</b>	
<b>12. DISTRIBUTION / AVAILABILITY STATEMENT</b>  Approved for Public Release; Distribution Unlimited			
<b>13. SUPPLEMENTARY NOTES</b>			

#### 14. ABSTRACT

**Purpose:** To develop a targeted T<sub>2</sub>-exchange MRI contrast agent for the early detection and diagnosis of prostate cancer.

**Scope:** This contrast agent is based on T<sub>2</sub> contrast (i.e., hypo-intense contrast) arising from water molecule exchange between the inner-sphere of a Dysprosium (Dy<sup>3+</sup>) central ion and the bulk water. The level of this "T<sub>2</sub>-exchange" contrast is highly dependent on both the water molecule exchange rate and the paramagnetic shift of the water molecule hydrogen protons when bound to the Dy<sup>3+</sup> ion. After identifying which DyDOTA-based chelate gave the optimal water molecule exchange rate at 9.4 T MRI, the chelate would then be polymerized to increase the transverse relaxivity (r<sub>2</sub>) per molecule by 100 fold. Thereby creating a highly sensitive, low molecular weight T<sub>2</sub> contrast agent for cancer molecular imaging with MRI. Polymers targeting the prostate specific membrane antigen (PSMA) of prostate cancer cells would then be synthesized and tested with both *in vitro* and *in vivo* experiments.

**Major Findings:** We found that the DyDOTA-(gly)<sub>2</sub> and DyDOTA-(gly)<sub>3</sub> chelates had almost ideal water molecule exchange rates at 9.4 T and 37 degrees Celsius, which gave them transverse relaxivities (r<sub>2</sub>) that were close to the theoretical maximum predicted by Swift-Connick theory. These two chelates were then chosen as candidates for polymerization. We also found that the paramagnetic shift in the bound water molecule hydrogen protons for each DyDOTA-based chelate was dependent on temperature. Details of these experiments and results are given in our Magnetic Resonance in Medicine publication. Unfortunately, polymerization of the DyDOTA-(gly)<sub>2</sub> and DyDOTA-(gly)<sub>3</sub> chelates proved to be extremely difficult, and only one version of the monomer chelates (DyDOTA) was successfully polymerized before the grant period ended. An alternate faster method could be to use dendrimers (n=16,32,64) instead of polymers to increase the total transverse relaxivity (r<sub>2</sub>) per molecule. We have asked for a 6 month long EWOFF to pursue this faster alternative approach that has more simplified chemistry.

#### 15. SUBJECT TERMS

MRI Contrast Agent, T2 contrast, Prostate Cancer, PSMA Targeted Agent, Early Detection and Diagnosis, Dysprosium (Dy<sup>3+</sup>) Paramagnetic Chelate, T2-exchange

#### 16. SECURITY CLASSIFICATION OF:

a. REPORT

Unclassified

b. ABSTRACT

Unclassified

c. THIS PAGE

Unclassified

#### 17. LIMITATION OF ABSTRACT

Unclassified

#### 18. NUMBER OF PAGES

21

#### 19a. NAME OF RESPONSIBLE PERSON USAMRMC

#### 19b. TELEPHONE NUMBER (include area code)

Standard Form 298 (Rev. 8-98)  
Prescribed by ANSI Std. Z39.18

## Table of Contents

	<u>Page</u>
<b>1. Introduction.....</b>	<b>5</b>
<b>2. Keywords.....</b>	<b>6</b>
<b>3. Accomplishments.....</b>	<b>6</b>
<b>4. Impact.....</b>	<b>10</b>
<b>5. Changes/Problems.....</b>	<b>11</b>
<b>6. Products.....</b>	<b>11</b>
<b>7. Participants &amp; Other Collaborating Organizations.....</b>	<b>12</b>
<b>8. Special Reporting Requirements.....</b>	<b>13</b>
<b>9. Appendices.....</b>	<b>13</b>

## 1. INTRODUCTION

### PC121497 Technical Abstract

The prostate-specific membrane antigen (PSMA), which is significantly over-expressed by prostate cancer cells, has proven to be an excellent target for imaging prostate cancer in mouse models, as recently shown for PSMA-targeted radiopharmaceuticals labeled with cysteineglutamate or lysine-glutamate ureas. Yet, dual-modality SPECT/CT and PET/CT imaging systems expose the subject to ionizing radiation, making them impractical for frequent therapeutic monitoring in patients. MRI systems offer superior anatomic resolution and soft tissue contrast compared to CT, making them an excellent tool for prostate cancer prevention studies. The effectiveness of MRI in the functional and molecular imaging regime is currently limited due to the lack of highly sensitive molecularly targeted contrast agents. Creating such agents would greatly improve the use of MRI for the early detection and diagnosis of prostate cancer. Our long-term goal is to use the newly described phenomena of T<sub>2</sub>-exchange to create targeted, highly sensitive, molecule-sized T<sub>2</sub> agents for contrast-enhanced molecular imaging of prostate cancer with MRI. It was recently shown that lanthanide-based Ln<sup>3+</sup>+DOTA chelates (Ln<sup>3+</sup> = La, Gd, Lu) create enhanced negative contrast (i.e., darkening) in MRI through the chemical exchange of water molecules. The level of this “T<sub>2</sub>-exchange” contrast, which adds to the inherent paramagnetic T<sub>2</sub> contrast of the Ln<sup>3+</sup> ion, is proportional to the bound water molecule chemical shift and reaches a maximum at a specific water molecule exchange rate. It was also recently demonstrated that T<sub>2</sub>-exchange contrast could be increased by several orders of magnitude through simple linear polymerization of the Ln<sup>3+</sup>+DOTA chelate. We hypothesize that by using these methods, a highly sensitive molecular imaging T<sub>2</sub> contrast agent with a transverse relaxivity (r<sub>2</sub>) an order of magnitude greater than any currently existing contrast agent (e.g., SPIO) can be created, while retaining the advantages of using small molecules rather than nanoparticles for improved biological targeting, uptake, and clearing. These agents have the potential to accurately image the location and size of cancerous lesions within the prostate, and (through PSMA as a prognostic indicator) differentiate between indolent and aggressive forms, thereby performing disease staging entirely non-invasively. Also, in contrast to PET/CT or SPECT/CT, disease diagnostics and therapy monitoring would be performed on a single-modality MRI instrument without the risk of exposure to ionizing radiation. This would reduce patient stress by increasing specificity and early detection, simplifying the imaging protocol, and reducing scan time.

### PC121497 Public Abstract

This research project will explore the idea of using a new chemical compound to help detect and image prostate cancer in the human body with magnetic resonance imaging (MRI). This method could allow prostate cancer to be detected at an earlier stage, determine its exact location within the prostate, and possibly even determine what type of prostate cancer it is. The chemical compound (also known as an MRI “contrast agent”) will be modified to attach itself to cancerous prostate cells but not to healthy prostate cells. In this way, the contrast agent would cause the cancer containing regions of the prostate to appear darker than the surrounding healthy tissue (that is, create “negative” contrast). This would allow the location of prostate cancer to be easily detected by

comparing MRI images from before and after administration of the intravenously injected contrast agent and looking for areas that appear darkened. This hypothesis will be tested by first evaluating both the contrast and cell-targeting capabilities of the contrast agent while outside the body (in vitro experiments), and then using mice bearing human prostate cancer tumors to evaluate the same capabilities when inside a body (in vivo experiments). If successful, this research could create a new class of highly sensitive, molecularly targeted MRI contrast agents for the early detection and diagnosis of prostate cancer. Also, in contrast to conventional PET/CT and SPECT/CT imaging, which use gamma rays and x-rays, MRI can be used for frequent therapeutic monitoring in patients without the harmful risks associated with ionizing radiation.

## 2. KEYWORDS

CT – x-ray computed tomography  
DOTA – 1,4,7,10-tetraazacyclododecane-1,4,7,10-tetraacetic acid  
Dy – Dysprosium  
Gd – Gadolinium  
Gly – Glycinate  
La – Lanthanum  
Ln – Lanthanide  
Lu - Lutetium  
MRI – Magnetic Resonance Imaging  
PET – Positron Emission Tomography  
PSMA – Prostate-Specific Membrane Antigen  
 $r_2$  – transverse relaxivity (sec-1mM-1)  
SCID – severe combined immunodeficiency  
SPECT – single photon emission computed tomography  
SPIO – super paramagnetic iron oxide nanoparticle  
 $T_2$  – transverse relaxation time (sec)

## 3. ACCOMPLISHMENTS

### - What were the major goals of the project?

From our Statement Of Work:

**Task 1.** Design and synthesis of a highly sensitive polymerized Dy<sup>3+</sup>+DOTA-based T2 contrast agent (months 1-6):

**1a.** First, we will maximize the T2-exchange contrast generated by the Dy<sup>3+</sup>+DOTA-based chelate by varying the water molecule exchange rate using several different DOTA sidearm structures (e.g., DOTA-, DOTA-(gly)2-, DOTA-(gly)4-). The maximum transverse relaxivity ( $r_2$ ) due to T2-exchange with a single Dy<sup>3+</sup> ion is theoretically 16 sec-1mM-1. Dr. Wu will perform the chemical synthesis while Dr. Soesbe will perform the in vitro  $r_2$  analysis (months 1-3).

**1b.** Once the ideal chemical structure/water molecule exchange rate has been determined, we will use the previously established polymerization method (3) to increase the level of T2 contrast by a factor of 20 to 100 times. If successful, the  $r_2$  from T2-exchange would then be 320 to 1600 sec-1mM-1 per molecule. Dr. Wu will perform the chemical synthesis while Dr. Soesbe will perform the in vitro  $r_2$  analysis (months 4-6).

**Task 2.** Create targeted versions of the polymerized T2 contrast agent and evaluate cell receptor binding characteristics with in vivo and in vitro experiments (months 6-12):

**2a.** We will create targeted versions of the of the polymerized T2-exchange contrast agent by attaching molecular targeting groups along the backbone of the linear polymer chain. One version will be labeled with biotin (for in vitro binding to streptavidin) while another version will be labeled with cysteine-glutamate or lysine-glutamate ureas (for in vivo binding to the prostate specific membrane antigen, or PSMA) (5). Dr. Wu will perform the chemical synthesis and analysis (months 6-8).

**2b.** The detection limit (and thus the sensitivity) of the targeted low molecular weight T2 contrast agent will be measured in vitro using the biotin labeled version of the polymer. A concentration array will be created using a small well plate, where each well will contain the same number of streptavidin coated agarose beads and the receptor concentration on the bead surface is precisely known. The level of T2 contrast in each well will be imaged using a small animal 9.4 T MRI system. Dr. Soesbe will perform the in vitro set up, MR imaging, and analysis (months 9-10).

**2c.** In vivo prostate cancer cell receptor binding will be evaluated using the cysteine-glutamate or lysine-glutamate urea labeled version of the polymer. The tumor uptake characteristics will be assessed by injecting the agent into SCID mice (8 total) bearing PSMA+ flank tumor xenografts (e.g., PC3-PIP) (1). The mice will then be imaged on a 9.4 T MRI system. The specificity and selectivity will be measured by using PSMA-xenografts (e.g., PC3-flu) within in the same mouse and by injecting the mice with a PSMA blocker (e.g., 2-(phosphonomethyl)pentanedioic acid) before administration of the contrast agent. Facility research staff will perform the tumor implantation while Dr. Soesbe will perform all in vivo imaging (months 11-12).

**- What was accomplished under these goals?**

**Task 1a. : Completed (3 months total)**

Four different versions of the DyDOTA-based chelate were synthesized (DyDOTA, DyDOTA-(gly)<sub>2</sub>, DyDOTA-(gly)<sub>3</sub>, and DyDOTA-(gly)<sub>4</sub>). Each chelate had a different number of glycinate (gly) side-arms (i.e., 0, 2, 3, or 4) and thus different water molecule exchange rates. Since T<sub>2</sub>-exchange is dependent on the water molecule exchange rate, each chelate had a different transverse relaxivity ( $r_2$ ) value. The non-water molecule exchanging chelate DyTETA was also synthesized in order to measure the transverse relaxivity ( $r_2$ ) due to the presence of the paramagnetic Dy<sup>3+</sup> ion itself (i.e., outer sphere relaxation). Both the transverse relaxivities ( $r_2$ ) and the water molecule exchange rates for

the five Dy<sup>3+</sup> chelates were measured *in vitro* on a vertical 400 MHz NMR system. These data were in excellent agreement with the theoretical values predicted by the Swift-Connick theory, proving this part of our hypothesis to be correct. These data showed that (at 9.4 T and 37 degrees Celsius) the water molecule exchange rate for DyDOTA was too fast, and that DyDOTA-(gly)<sub>4</sub> was too slow, but that both DyDOTA-(gly)<sub>2</sub> and DyDOTA-(gly)<sub>3</sub> had exchange rates that placed them close to the maximum  $r_2$  value. Therefore, DyDOTA-(gly)<sub>2</sub> and DyDOTA-(gly)<sub>3</sub> were selected as candidates for polymerization. Further details for this completed task (including *in vitro* images) can be found in our Magnetic Resonance in Medicine publication, which is included in the Appendix at the end of this report.

#### **Task 1b. : Attempted, but not completed (9 months, estimated time was 3 months)**

At project month 4 we started synthesizing the polymers, but polymerization of the DyDOTA-(gly)<sub>2</sub> and DyDOTA-(gly)<sub>3</sub> chelates proved to be far more challenging than initially anticipated. Under the guidance of Dr. Yunkou Wu (Faculty), Lei Zhang (Undergraduate Research Assistant) attempted to synthesize the polymers. He found difficulty in producing the final compounds due to the incompatibility of our synthetic methods with the stability of the polymer. When we attempted the polymerization with the metallated monomers, we found that solubility issues limited our polymerization efficiency. This was due to the charge on the monomer being highly cationic. When we then used the organic framework *without* the lanthanide ion during polymerization, we were successful and resulted in a high efficiency of polymerization (up to ~100 units). Unfortunately, during subsequent metallation of the of the ~100 unit organic polymer we observed cleavage of the peptide backbone due to the acidity of the lanthanide ions and their kinetic affinity to carbonyls. In other words, the polymer backbone fell apart. This was apparent as chemical analysis observed a series of lower molecular weight molecules that were consistent with degradation of a larger molecular weight polymer. We were able to overcome this degradation (by Dr. Wu, see below) with the addition of citrate during metallation, which was used to limit the kinetically favorable chelation along the backbone and to allow for the thermodynamically favorable chelation by the macrocycle unit.

At project month 11 (December 2014), Mr. Zhang stopped working on this research project and all polymerization attempts were continued by Dr. Yunkou Wu directly. By using Lei Zhang's starting materials, Dr. Wu was able to synthesize the DyDOTA version of the polymer within two weeks time. Initial characterization showed the polymer backbone length to be approximately 100 units with about 50% population of DyDOTA. Therefore the transverse relaxivity ( $r_2$ ) of this molecule should be 50 times that of the monomer chelate. While the water molecule exchange rate of DyDOTA is not ideal (too fast) for maximizing  $T_2$ -exchange at 9.4 T and 37 degrees Celsius, this nonetheless proved that polymerization of the DyDOTA-based chelates was indeed possible. At project month 12 two things happened 1) Our Lead Chemist Dr. Wu left UT Southwestern, and 2) our 12-month long grant period was up. Therefore no further chemistry was completed on this project.



After speaking with Dr. Mark Milne (Postdoctoral researcher) we decided to ask for a 6 to 12-month long EWOFF to complete Task 1b as well as some aspects of Task 2 (specifically *in vitro* and *in vivo* imaging of the non-targeted agent). Since polymerization of the remaining DyDOTA-based chelates would require synthesizing new starting materials, and since Dr. Wu (our polymerization expert) is no longer at our institution, we have decided to use dendrimers to create multiple DyDOTA-based molecules instead of polymers. This will greatly simplify the required chemistry as the dendrimer backbones ( $n = 32, 64, 128$ ) can be simply purchased (e.g., from Sigma Aldrich). Also, substituting dendrimers for polymers does not change the research goals of our initial Statement Of Work (SOW). During the proposed EWOFF we will create DyDOTA-(gly)<sub>2</sub> and DyDOTA-(gly)<sub>3</sub> dendrimers ( $n = 64$ ), perform *in vitro* characterization and imaging, and initial *in vivo* imaging. Since the dendrimers will be non-targeted, we can use the collection by the mouse kidneys to determine the *in vivo* T<sub>2</sub>-exchange contrast capabilities, similar to our previous publications.

**Task 2a, 2d, and 2c: Not completed**

Since these tasks depended on successful polymerization of the monomer chelates, which took much longer than expected (> 9 months), they could not be completed in time

**- What opportunities for training and professional development have the project provided?**

**Todd C. Soesbe, Ph.D.**

**Training:** Dr. Soesbe had to learn O-17 NMR spectroscopy and Matlab fitting in order to measure the water molecule exchange rates of the DyDOTA-based monomers.

**Professional Development:** Dr. Soesbe held bi-weekly lab group meetings to help with collaboration among the group members. He also gave two conference presentations (see Section 6) about this research where he discussed similar research with peers.

**Yunkou Wu, Ph.D.**

**Training:** Dr. Wu received training on how to operate the Agilent 9.4 T animal MRI system from Dr. Soesbe.

**Professional Development:** Dr. Wu attended the bi-weekly lab group meetings to discuss aspects of the current project, present results, and review current and previous literature.

**Mark Milne, Ph.D.**

**Training:** Dr. Milne received training from Dr. Wu on polymer chemistry and synthesis methods. He also received training from Dr. Ratnakar on dendrimer chemistry and synthesis.

**Professional Development:** Dr. Milne attended the bi-weekly lab group meetings to discuss aspects of the current project, present results, and review current and previous literature.

**Lei Zhang**

**Training:** Mr. Zhang received training from Dr. Wu on polymer chemistry and synthesis methods.

**Professional Development:** Mr. Zhang attended the bi-weekly lab group meetings to discuss aspects of the current project, present results, and review current and previous literature.

**- How were the results disseminated to the community of interest?**

Along with our Magnetic Resonance in Medicine publication, Dr. Soesbe presented these data at several conferences for peer evaluation and education. He also used these data to discuss “current exciting research” when making presentations at UT Southwestern to summer undergraduate research students and teachers (i.e., the UT Southwestern SURF and STARS programs) and to graduate school candidates for the UT Southwestern Biomedical Engineering graduate program.

**- What do you plan to do during the next reporting period to accomplish the goals?**

Nothing to report, as this is the Final Report.

#### **4. IMPACT**

**- What was the impact on the development of the principal discipline(s) of the project?**

Although  $T_2$  contrast by  $T_2$ -exchange has existed in NMR and MRI for over 30 years, until our research, no one has truly understood the dependence on proton exchange either through  $-NH$  and  $-OH$  bonds or  $H_2O$  exchange. Also, until our research, no one has ever attempted to maximize paramagnetic  $T_2$ -exchange by modulating the water molecule exchange rate using chelate structure. Our success with the monomer DyDOTA-based chelates (as described in our MRM publication, see Appendix) opens up a new modality for generating  $T_2$  contrast in magnetic resonance imaging.  $T_2$ -exchange differs from conventional  $T_2^*$  contrast mechanisms (such as super-paramagnetic iron oxide nanoparticles, i.e. SPIO) in that it does not rely on magnetic susceptibility to shorten  $T_2$  times. Therefore, susceptibility-based image artifacts are non-existent with  $T_2$ -exchange contrast agents. Also, when compared to SPIO, polymerized or dendrimerized  $T_2$ -exchange contrast agents are molecule-sized and not nanoparticle sized. This enhances the potential application of  $T_2$ -exchange contrast agents for molecular imaging in MRI, where effective agent uptake and targeting are crucial. Since our 2014 publication, there has already been another  $T_2$ -exchange publication in MRM by another group (NH Yadav, et al., Magn Reson Med, 72:823-828, 2014) describing the use of D-Glucose as a diamagnetic  $T_2$ -exchange agent, as well as another groups  $T_2$ -exchange publication that is currently in review by Magnetic Resonance in Medicine. It is anticipated that  $T_2$ -exchange contrast will become an important tool for contrast-enhanced imaging with magnetic resonance.

**- What was the impact on other disciplines?**

Nothing to report.

**- What was the impact on technology transfer?**

Nothing to report.

**- What was the impact on society beyond science and technology?**

Nothing to report.

**5. CHANGES/PROBLEMS**

**- Changes in approach and reasons for change.**

Although polymerization of the DyDOTA-based chelates was shown to be possible, it was also very time consuming and greatly inhibited our progress for this 12-month long grant. As an alternate approach we have suggested using a dendrimers structure (n = 32, 64, or 128) for the multiple DyDOTA chelate backbone. Since dendrimer backbones can simple be purchased (e.g., Sigma Aldrich), this will greatly simplify the chemistry required for synthesis, and greatly speed up the project, without changing the overall goals of our Statement of Work. We have suggested this path for our applied EWOFF.

**- Actual or anticipated problems or delays and actions or plans to resolve them.**

Please see previous statement.

**6. PRODUCTS**

**- Peer-Reviewed Journal Publications (see Appendix for full article copy)**

**Authors:** Todd C. Soesbe, S. James Ratnakar, Mark Milne, Shanrong Zhang, Quyen N. Do, Zoltan Kovacs, and A. Dean Sherry

**Title:** Maximizing T2-exchange in Dy<sup>3+</sup>+DOTA-(amide)<sub>x</sub> chelates: fine-tuning the water molecule exchange rate for enhanced T2 contrast in MRI

**Journal:** Magnetic Resonance in Medicine

**Volume:** 71

**Date:** March 2014

**Page numbers:** 1179-1185

**Status of publication:** published

**Acknowledgment of federal support:** yes

**- Peer-Reviewed Conference Presentations (see Appendix for abstract copies)**

**Date:** April 3, 2014

**Presenter:** Todd C. Soesbe, Ph.D.

**Presentation type:** Oral

**Presentation title:** Contrast, paramagnetism, and their applications in MRI  
**Host:** UT Southwestern Medical Center at Dallas and The University of Texas at Dallas  
Joint Biomedical Engineering Graduate Program, Retreat & Scientific Symposium  
**Location:** Dallas, Texas

**Date:** November 8, 2014

**Presenter:** Todd C. Soesbe, Ph.D.

**Collaborators:** James Ratnakar, Mark Milne, Fiemu Nwariaku, A. Dean Sherry, and Robert E. Lenkinski

**Presentation type:** Oral

**Presentation title:** Advancing the early detection and diagnosis of primary and recurring thyroid cancers using a molecularly targeted T2-exchange MRI contrast agent

**Host:** International Society of Magnetic Resonance in Medicine, Workshop Series 2014: Magnetic resonance in cancer: challenges and unmet needs

**Location:** Austin, Texas

## **7. PARTICIPANTS & OTHER COLLABORATING ORGANIZATIONS**

### **- What individuals have worked on the project?**

**Name:** Todd C. Soesbe, Ph.D. (Principal Investigator)

**Project role:** Faculty, Physicist and MR Imaging Specialist

**Researcher identifier (UT Southwestern ID):** 56841

**Nearest person month worked:** 6

**Contribution to project:** Dr. Soesbe served as Principal Investigator for this project by organizing and driving the research and performing all imaging experiments.

**Funding support:** UT Southwestern Medical Center

**Name:** Yunkou Wu, Ph.D.

**Project role:** Faculty, Lead Chemist

**Researcher identifier (UT Southwestern ID):** 121991

**Nearest person month worked:** 3

**Contribution to project:** Dr. Wu served as the principal chemist for this project and was responsible for synthesis, polymerization, and characterization of the Dy<sup>3+</sup>+DOTA-based ligands.

**Funding support:** UT Southwestern Medical Center

**Name:** Mark Milne, Ph.D.

**Project role:** Postdoctoral Researcher, Chemist

**Researcher identifier (UT Southwestern ID):** 145045

**Nearest person month worked:** 1

**Contribution to project:** Dr. Milne assisted Dr. Wu with the synthesis and polymerization of the Dy<sup>3+</sup>+DOTA-based ligands and will be responsible for synthesizing the dendrimers version of the Dy<sup>3+</sup>+DOTA chelates during the requested EWOFF.

**Funding support:** UT Southwestern Medical Center

**Name:** Lei Zhang

**Project role:** Undergraduate Research Assistant, Chemist

**Researcher identifier (UT Southwestern ID):** 133372

**Nearest person month worked:** 2

**Contribution to project:** Mr. Zhang assisted Dr. Wu with the synthesis and polymerization of the Dy3+DOTA-based ligands.

**Funding support:** The University of Texas at Dallas

**- Has there been a change in the active other support of the PD/PI(s) or senior/key personnel since the last reporting period?**

Nothing to report.

**- What other organization were involved as partners?**

Nothing to report.

## **8. SPECIAL REPORTING REQUIREMENTS**

Nothing to report.

## **9. APPENDECIES**

- MRM publication
- ISMRM cancer workshop abstract

# Maximizing $T_2$ -Exchange in $Dy^{3+}$ DOTA-(amide)<sub>x</sub> Chelates: Fine-Tuning the Water Molecule Exchange Rate for Enhanced $T_2$ Contrast in MRI

Todd C. Soesbe,<sup>1,2\*</sup> S. James Ratnakar,<sup>1</sup> Mark Milne,<sup>3</sup> Shanrong Zhang,<sup>1</sup> Quyen N. Do,<sup>4</sup> Zoltan Kovacs,<sup>1,4</sup> and A. Dean Sherry<sup>1,2,4</sup>

**Purpose:** The water molecule exchange rates in a series of DyDOTA-(amide)<sub>x</sub> chelates were fine-tuned to maximize the effects of  $T_2$ -exchange line broadening and improve  $T_2$  contrast.

**Methods:** Four DyDOTA-(amide)<sub>x</sub> chelates having a variable number of glycinate side-arms were prepared and characterized as  $T_2$ -exchange agents. The nonexchanging DyTETA chelate was also used to measure the bulk water  $T_2$  reduction due solely to  $T_2^*$ . The total transverse relaxivity ( $r_{2tot}$ ) at 22, 37, and 52°C for each chelate was measured in vitro at 9.4 Tesla (400 MHz) by fitting plots of total  $T_2^{-1}$  versus concentration. The water molecule exchange rates for each complex were measured by fitting  $^{17}O$  line-width versus temperature data taken at 9.4 Tesla (54.3 MHz).

**Results:** The measured transverse relaxivities due to water molecule exchange ( $r_{2ex}$ ) and bound water lifetimes ( $\tau_M$ ) were in excellent agreement with Swift-Connick theory, with DyDOTA-(gly)<sub>3</sub> giving the largest  $r_{2ex} = 11.8 \text{ s}^{-1} \text{ mM}^{-1}$  at 37°C.

**Conclusion:** By fine-tuning the water molecule exchange rate at 37°C, the transverse relaxivity has been increased by 2 to 30 times compared with previously studied  $Dy^{3+}$ -based chelates. Polymerization or dendrimerization of the optimal chelate could yield a highly sensitive, molecule-sized  $T_2$  contrast agent for improved molecular imaging applications. **Magn Reson Med 71:1179–1185, 2014. © 2014 Wiley Periodicals, Inc.**

**Key words:** MRI;  $T_2$  contrast;  $T_2$ -exchange; water molecule exchange; in vitro; Dysprosium(III)

## INTRODUCTION

### Contrast in MR Imaging

MRI can be used to create a three-dimensional image representing the water proton ( $^1H$ ) density within a subject (1,2). Because the human body is approximately 70% water, most tissues have a sufficiently large water proton signal to allow for high-resolution anatomical imaging. The contrast between different soft tissue types, which results in some tissues appearing brighter or darker than others, depends upon both the endogenous proton density and the  $T_1$  and  $T_2$  relaxation times (3). MRI tissue contrast can be further enhanced by introducing an exogenous contrast agent (4). These agents shorten the endogenous  $T_1$  and  $T_2$  relaxation times of tissue water to enhance the contrast and highlight specific anatomic features or dynamic processes.

The most widely used MRI contrast agents consist of various chelated forms of  $Gd^{3+}$  where the central ion is surrounded by a multidentate ligand that typically occupies eight of nine possible coordination positions (5,6).  $Gd^{3+}$  is most effective at relaxing water protons because this ion has seven unpaired electrons distributed isotropically in the 4f orbitals ( $^8S_{7/2}$ ) and an electron relaxation rate that is approximately  $10^6$  times slower than any other lanthanide ion (7). This reduced electron relaxation rate is more in tune with the typical Larmor frequencies of  $^1H$  protons in MRI ( $\omega = \gamma B_0$ ) and, therefore, enhances the mechanism of electron to proton dipole-dipole relaxation (8). The relaxation efficiency of  $Gd^{3+}$  also depends upon the rapid chemical exchange of water molecules between a single inner-sphere coordination position of  $Gd^{3+}$  ion and bulk water. Although  $Gd^{3+}$  shortens both the  $T_1$  and  $T_2$  of water protons, the  $T_1$  effects are more pronounced because the  $T_1$  of tissue water protons are approximately an order of magnitude longer than  $T_2$ . Hence, for most common imaging sequences, a typical clinical dose of  $Gd^{3+}$  agent (e.g., 0.1 mmol/kg) will cause tissue regions of uptake to appear brighter than the surrounding tissue. Nonetheless, the effects of  $T_2$  shortening (image darkening) can be observed in tissues (such as the kidneys) where  $Gd^{3+}$  accumulates in high concentrations.

Other lanthanide ions such as  $Tb^{3+}$ ,  $Dy^{3+}$ , and  $Ho^{3+}$  have fewer unpaired electrons distributed anisotropically in the 4f orbitals and relatively rapid electron relaxation rates compared with  $Gd^{3+}$ . These faster rates, combined with larger

<sup>1</sup>Advanced Imaging Research Center, UT Southwestern Medical Center, Dallas, Texas, USA.

<sup>2</sup>Department of Radiology, UT Southwestern Medical Center, Dallas, Texas, USA.

<sup>3</sup>Department of Chemistry, University of Western Ontario, London, Ontario, Canada.

<sup>4</sup>Department of Chemistry, University of Texas, Dallas, Texas, USA.

Grant sponsor: National Institutes of Health; Grant number: CA-115531, CA-126608; Grant sponsor: Robert A. Welch Foundation; Grant number: AT-584.

\*Correspondence to: Todd C. Soesbe, Ph.D., Advanced Imaging Research Center, University of Texas Southwestern Medical Center, 5323 Harry Hines Boulevard, Dallas, TX 75390-8568. E-mail: todd.soesbe@utsouthwestern.edu  
Additional Supporting Information may be found in the online version of this article.

Received 20 August 2013; revised 24 November 2013; accepted 2 December 2013

DOI 10.1002/mrm.25091

Published online 3 January 2014 in Wiley Online Library (wileyonlinelibrary.com).

© 2014 Wiley Periodicals, Inc.

magnetic moments (7), make these ions more effective as  $T_2^*$  agents. This susceptibility-based  $T_2$  relaxation mechanism is due to the magnetic moments of the  $\text{Ln}^{3+}$  ions causing local  $B_0$  inhomogeneities in their immediate vicinity ( $\approx 15$  Å diameter) (7). Water molecule protons either directly bound to the  $\text{Ln}^{3+}$  ion (i.e., inner-sphere relaxation) or within the vicinity of the  $\text{Ln}^{3+}$  ion (i.e., outer-sphere relaxation) experience an altered  $B_0$  field and precess at a different Larmor frequency ( $\omega = \gamma(B_0 \pm \Delta B)$ ). These different Larmor frequencies result in increased spin de-phasing in the plane transverse to  $B_0$  and thus shorter effective  $T_2$  times. In this way, certain paramagnetic chelates can act as susceptibility or  $T_2^*$  agents in a manner similar to superparamagnetic iron oxide nanoparticles (9). Furthermore, unlike  $\text{Gd}^{3+}$ , the remaining paramagnetic lanthanides ions can induce large hyperfine shifts in all chelate protons including those in exchange with water protons (i.e.,  $-\text{NH}$  and  $-\text{OH}$  protons and any inner-sphere water molecules) (10–12). This hyperfine shift ( $\Delta\omega$ ) has led to the development of two relatively new MRI contrast mechanisms: chemical exchange saturation transfer (CEST) (13) and  $T_2$ -exchange ( $T_{2\text{ex}}$ ). While the former has been recently reviewed in depth elsewhere (14,15), the latter is discussed in more detail in the following section.

### $T_2$ -exchange Theory and Background

It was recently shown that the same intermediate water molecule exchange rates that facilitate paramagnetic chemical exchange saturation transfer (paraCEST) (16) between the inner-sphere of  $\text{EuDOTA}(\text{amide})_4$  chelates and bulk water can also significantly reduce the bulk water  $T_2$  through a  $T_{2\text{ex}}$  mechanism (17). The  $T_{2\text{ex}}$  contribution of these  $\text{Eu}^{3+}$ -based agents can be quite substantial even though the  $\text{Eu}^{3+}$  ion is only weakly paramagnetic (18).  $T_{2\text{ex}}$  is caused by mobile proton exchange between the chelate and the bulk water. This proton exchange can occur through exchangeable  $-\text{NH}$  and  $-\text{OH}$  protons on the ligand and through water molecule exchange with the inner-sphere of the  $\text{Ln}^{3+}$  ion. The  $T_{2\text{ex}}$  mechanism, which is independent of the CEST saturation pulse, is a function of the agent concentration (mM), the number of proton or water molecule exchange sites ( $q$ ), the bound proton chemical shift ( $\Delta\omega$ ), and most importantly the proton or water molecule exchange rates ( $k_{\text{ex}}$ ). It has also been shown that the transverse relaxivity caused by  $T_{2\text{ex}}$  (i.e.,  $r_{2\text{ex}}$ ) reaches a peak value for a given  $B_0$  at a specific exchange rate defined by  $k_{\text{ex}} = \Delta\omega$ , where  $\Delta\omega$  is expressed in  $\text{rad s}^{-1}$  (17,19,20).

Diamagnetic  $T_{2\text{ex}}$  from compounds with exchanging  $-\text{NH}$  or  $-\text{OH}$  protons (e.g.,  $\text{NH}_4\text{Cl}$ ) has long been used for bulk water solvent signal suppression in high-resolution NMR experiments (21,22), and has more recently been proposed as an exogenous  $T_2$  contrast mechanism for MRI (23,24). However, diamagnetic  $T_{2\text{ex}}$  agents require high concentrations (e.g., 500 mM) to achieve significant bulk water  $T_2$  reduction and negative contrast, making them impractical for in vivo applications. The  $T_{2\text{ex}}$  effect can be greatly increased by using inner-sphere water molecule exchange in chelates containing paramagnetic  $\text{Ln}^{3+}$  ions. This was originally demonstrated by Aime et al (25) where it was shown that the amount of  $\text{DyDOTA}(\text{mono-amide})$  required to suppress the bulk water peak in high-resolution NMR experiments was reduced by a factor of 200 (from 500 mM to 2.5 mM). This increase in  $T_{2\text{ex}}$  sensitivity is mainly due to the increase in  $\Delta\omega$  when moving

from diamagnetic  $-\text{NH}$  and  $-\text{OH}$  proton exchange (where  $\Delta\omega$  is typically 2 to 5 ppm) to paramagnetic  $\text{Ln}^{3+}$  inner-sphere water molecule exchange (where  $\Delta\omega$  can range from 50 ppm for  $\text{Eu}^{3+}$  to 800 ppm for  $\text{Dy}^{3+}$ ) (11). It is important to note that the reduction in the bulk water  $T_2$  due to  $T_{2\text{ex}}$  is *in addition* to the paramagnetic line broadening caused by the  $\text{Ln}^{3+}$  ion itself ( $T_{2\text{para}}$ ). This makes some of the  $\text{Ln}^{3+}$  ions (most notably  $\text{Dy}^{3+}$ ) strong candidates for development into highly sensitive  $T_2$  contrast agents for MRI.

In fact, some chelates containing the  $\text{Dy}^{3+}$  ion have previously been pursued as  $T_2$  contrast agents. The most well-known example being  $\text{DyDTPA-BMA}$  or  $\text{Sprodiamide}^{\text{TM}}$  (Nycomed, UK) (26), the  $\text{Dy}^{3+}$  analog of the nonionic  $\text{GdDTPA-BMA}$  or  $\text{gadodiamide}$  (i.e.,  $\text{Omniscan}^{\text{TM}}$ ; Nycomed, UK).  $\text{DyDTPA-BMA}$  was first assessed for demarcation of myocardial ischemia (26–30), tumor tissue characterization (31), and even Phase I clinical trials for cerebral perfusion imaging (32). These in vivo examples illustrate the many possible applications for a small molecule-sized  $T_2$  MRI contrast agent. Other previous  $\text{Dy}^{3+}$ -based chelate studies include  $\text{DyDTPA}$ -based derivatives and starch microparticles (19,33,34),  $\text{DyDOTA}$ -based monomers and dendrimers (25,33,35), and the MS-325 human serum albumin binding ligand (20). It is important to note that for these previous  $\text{Dy}^{3+}$  chelates the water molecule exchange rates at  $37^\circ\text{C}$  were either too fast or too slow to maximize  $r_{2\text{ex}}$ , typically being one to two orders of magnitude away from the ideal exchange rate defined by  $k_{\text{ex}} = \Delta\omega$  (19,33). Interestingly, several of the early studies on  $\text{Dy}^{3+}$  chelates did observe that their total transverse relaxivity ( $r_{2\text{tot}}$ ) was indeed proportional to the water molecule exchange rate ( $k_{\text{ex}}$ ) and bound water chemical shift ( $\Delta\omega$ ). This was demonstrated by varying the chemical structure, temperature, and  $B_0$  field (19,20,25,33), and was elegantly explained in theoretical detail by Caravan et al (20). Although the concept of maximizing the transverse relaxivity for a  $\text{Dy}^{3+}$ -based chelate by adjusting the water molecule exchange to the ideal rate had been proposed, to the best of our knowledge it has not been previously implemented.

### Hypothesis and Objectives

In this study, Swift-Connick theory (17,19,20) was used to optimize the transverse relaxivity produced by a series of  $\text{DyDOTA}(\text{amide})_x$  systems at  $37^\circ\text{C}$ . This was achieved by modulating the water molecule exchange rate with different DOTA ligand side-arm structures, and by maximizing  $\Delta\omega$  with magnetic field strength ( $B_0 = 9.4$  Tesla [T]). The  $\text{DyDOTA}(\text{amide})_x$  chelate structure that gave the ideal exchange rate at 400 MHz (9.4T) and  $37^\circ\text{C}$  was determined by in vitro  $T_2$  measurements, and the water molecule exchange rates for each chelate were confirmed using variable temperature  $^{17}\text{O}$  line-width measurements. Based on these results, one can hypothesize that polymerized or dendrimerized versions of these  $\text{DyDOTA}(\text{amide})_x$  chelates could create a new class of highly sensitive  $T_2$  contrast agents for MRI.

## METHODS

### Chelate Synthesis

Five different  $\text{Dy}^{3+}$  chelates were synthesized (Fig. 1), each having a different water molecule exchange rate. Four of the chelates (a–d) used the DOTA ligand (1,4,7,10-tetraazacyclododecane-1,4,7,10-tetraacetic acid) and one (e) used the



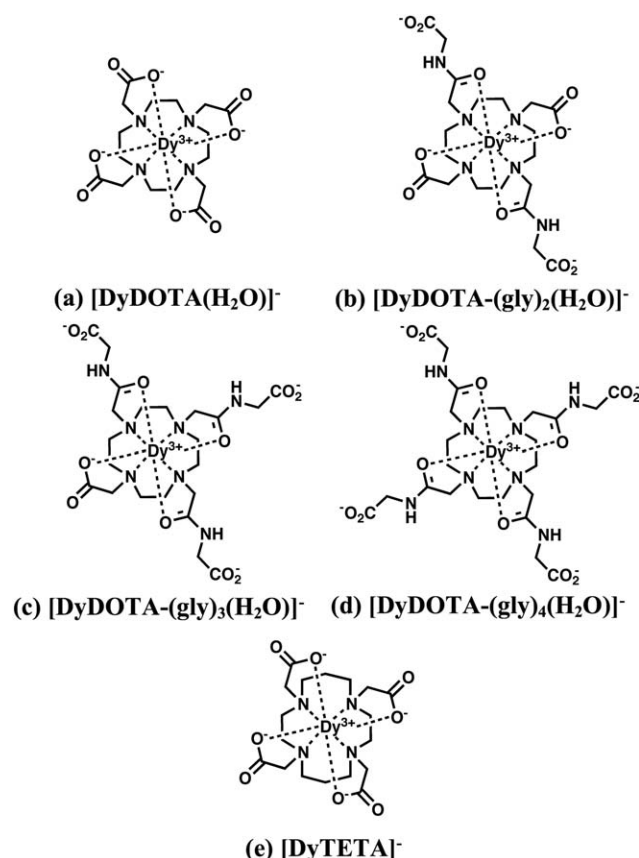


FIG. 1. Chemical structures of the five  $\text{Dy}^{3+}$  chelates used in this study. The four  $\text{DyDOTA}(\text{amide})_x$  chelates (a–d) have varying inner-sphere water molecule exchange rates, while the  $\text{DyTETA}$  chelate (e) has no water molecule exchange and therefore no  $T_{2\text{ex}}$  effects on the bulk water  $T_2$ .

TETA ligand (1,4,8,11-tetraazacyclotetradecane-1,4,8,11-tetraacetate). The four  $\text{DOTA}(\text{amide})_x$  ligands were synthesized according to earlier published methods (36–38), while the TETA ligand was purchased from Sigma-Aldrich (St. Louis, MO). All five  $\text{Dy}^{3+}$  complexes were prepared by reacting the corresponding free ligand with  $\text{DyCl}_3$  in water at pH 6.0 and  $25^\circ\text{C}$  for 24 h. The absence of any free  $\text{Dy}^{3+}$  metal was confirmed using the Xylenol Orange indicator test, and the concentration of  $\text{Dy}^{3+}$  in each complex was measured using ICP-OES analysis.

The water molecule exchange rates of the four  $\text{DOTA}(\text{amide})_x$  chelates were inversely proportional to the number glycinate side-arm structures ( $\text{NHCH}_2\text{COO}^-$ ) attached to the DOTA ring (i.e., 0, 2, 3, or 4). Therefore, the water molecule exchange rate ranged from fast for  $\text{DyDOTA}$ , to slower with additional glycinate amide groups, to slowest for  $\text{DyDOTA}-(\text{gly})_4$ . The  $\text{DyTETA}$  chelate, while structurally similar to  $\text{DyDOTA}$ , lacks an inner-sphere water molecule and cannot by definition have a  $T_{2\text{ex}}$  contribution to the water line-width. Hence, this chelate served as a useful control to measure the changes in the bulk water  $T_2$  due solely to the paramagnetic effects of the  $\text{Dy}^{3+}$  ion (i.e., outer-sphere relaxation only).

### In Vitro Experiments

The total transverse relaxivity ( $r_{2\text{tot}}$ ) was measured as a function of temperature for each of the five  $\text{Dy}^{3+}$  chelates.

This was performed by creating a concentration array for each chelate (0.125, 0.25, 0.5, and 1.0 mM) in 5 mm NMR tubes, with each sample adjusted to a pH of 7.0. The total  $T_2$  ( $T_{2\text{tot}}$ ) for each sample was then measured on an Agilent (Santa Clara, CA) 400 MHz NMR system using the Carr-Purcell-Meiboom-Gill pulse sequence. The  $T_{2\text{tot}}$  data were acquired at 22, 37, and  $52^\circ\text{C}$  for each chelate to determine how the  $r_{2\text{tot}}$  varied as a function of water molecule exchange rate. The  $r_{2\text{tot}}$  values (in units of  $\text{s}^{-1} \text{mM}^{-1}$ ) were calculated by plotting  $T_{2\text{tot}}^{-1}$  versus  $\text{Dy}^{3+}$  concentration and using the slope of the least squares fitted line. The transverse relaxivity due to water molecule exchange ( $r_{2\text{ex}}$ ) for each  $\text{DyDOTA}(\text{amide})_x$  chelate was then calculated by subtracting the total transverse relaxivity of  $\text{DyTETA}$  from  $r_{2\text{tot}}$  (i.e.,  $r_{2\text{ex}} = r_{2\text{tot}} - r_{2\text{DyTETA}}$ ) at each temperature. The measurement error in  $r_{2\text{tot}}$  from the least squares fitting was less than 10% and the  $\text{Dy}^{3+}$  concentration of each sample was verified by ICP-OES analysis.

The water molecule exchange rate for each  $\text{Dy}^{3+}$  chelate was calculated by measuring the variation in the  $^{17}\text{O}$  peak line-width as a function of temperature. Aqueous samples of each chelate (18 mM  $[\text{Dy}^{3+}]$ , pH 7.0, and enriched to 2%  $^{17}\text{O}$ ) were loaded into 18  $\mu\text{L}$  spherical capillaries from Wilmad-LabGlass (Vineland, NJ) to remove any susceptibility effects and then placed inside thin-walled, water-filled 5 mm NMR tubes also from Wilmad-LabGlass. An Agilent 400 MHz NMR system was used to measure the  $^{17}\text{O}$  line-width (TR = 250 ms, acquisition time = 80 ms, 128 averages) as the temperature was varied from 5 to  $90^\circ\text{C}$  in  $5^\circ\text{C}$  steps (18 points). The change in transverse relaxation rate due to exchange ( $T_{2\text{ex}}^{-1}$ ) as a function of temperature (i.e., water molecule exchange rate) was calculated by first converting the line-width data ( $T_{2\text{tot}}^{-1} = \pi \times \text{line-width}$ ) then subtracting the  $\text{DyTETA}$  data ( $T_{2\text{ex}}^{-1} = T_{2\text{tot}}^{-1} - T_{2\text{DyTETA}}^{-1}$ ). The water molecule exchange rates were then calculated by fitting the temperature dependant  $T_{2\text{ex}}^{-1}$  data with a model given by Pubanz et al (39) and the MATLAB non-linear least squared algorithm (Natick, MA). The measurement error in  $\tau_M$  ( $\pm$  one standard deviation) was estimated to be less than 20%.

*In vitro* images of the five  $\text{Dy}^{3+}$  chelate samples, along with a pure water standard, were acquired simultaneously on an Agilent (Santa Clara, CA) 9.4T (400 MHz) small animal MRI system using standard 5 mm diameter HPLC glass tubes and a 38 mm diameter  $^1\text{H}$  birdcage volume coil. Each sample was approximately 200  $\mu\text{L}$  with a  $\text{Dy}^{3+}$  concentration of 20 mM and a pH of 7.0. The sample temperature was monitored with a thermocouple and held constant by a heated air system from Small Animal Instruments (Stony Brook, NY). The fast spin-echo settings were: TR/TE = 2500/12.4 ms, echo train = 8, averages = 8, field of view =  $64 \times 16 \times 5$  mm, matrix =  $512 \times 128 \times 1$  pixels, with an image scan time of 5 m 25 s.

## RESULTS

### In Vitro Results

A plot of  $T_{2\text{tot}}^{-1}$  versus  $\text{Dy}^{3+}$  concentration is shown in Figure 2 for  $\text{DyDOTA}-(\text{gly})_2$  at 22, 37, and  $52^\circ\text{C}$ . The slope of each least squares fitted line gives the calculated  $r_{2\text{tot}}$  at that temperature. Figure 2 shows that  $r_{2\text{tot}}$



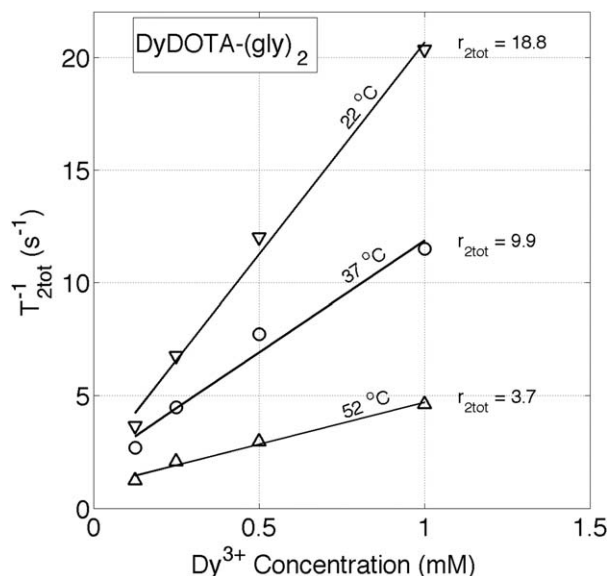


FIG. 2. A plot of total transverse relaxation rate ( $T_{2\text{tot}}^{-1}$ ) versus  $\text{Dy}^{3+}$  concentration for the  $\text{DyDOTA}(\text{gly})_2$  chelate at 22, 37, and 52°C. The slope of the least square fitted lines gives the total transverse relaxivity ( $r_{2\text{tot}}$ ) at that temperature. Measurement error for  $r_{2\text{tot}}$  was less than 10%.

decreases with increasing temperature indicating that, within this temperature range, slower water molecule exchange rates ( $k_{\text{ex}}$ ) give higher total relaxivity values for  $\text{DyDOTA}(\text{gly})_2$ . The similarly measured  $r_{2\text{tot}}$  values for all five  $\text{Dy}^{3+}$  chelates studied are summarized in Table 1, which also shows the calculated  $r_{2\text{ex}}$  values (i.e.,  $r_{2\text{ex}} = r_{2\text{tot}} - r_{2\text{DyTETA}}$ ) for each temperature. Table 1 shows that over the given temperature range,  $r_{2\text{tot}}$  and  $r_{2\text{ex}}$  are inversely proportional to temperature for  $\text{DyDOTA}$  and  $\text{DyDOTA}(\text{gly})_2$  yet are proportional to temperature for  $\text{DyDOTA}(\text{gly})_3$  and  $\text{DyDOTA}(\text{gly})_4$ . Note that for  $\text{DyTETA}$ , which has no water molecule exchange, the  $r_{2\text{tot}}$  is relatively independent of temperature. Also included in Table 1 are the bound water lifetimes ( $\tau_M = k_{\text{ex}}^{-1}$ ) at 22, 37, and 52°C that were calculated from the variable-temperature  $^{17}\text{O}$  data. Figure 3 shows a plot of the  $^{17}\text{O}$  measured  $T_{2\text{ex}}^{-1}$  versus temperature for  $\text{DyDOTA}(\text{gly})_4$  (raw data shown as circles). The Matlab fit to these data, based on Eq. [1] in Pubanz et al (39), gave values for  $k_{\text{ex}}^{298}$  and  $\Delta H^\ddagger$  which were used to calculate  $\tau_M$  at each temperature using the equation below:

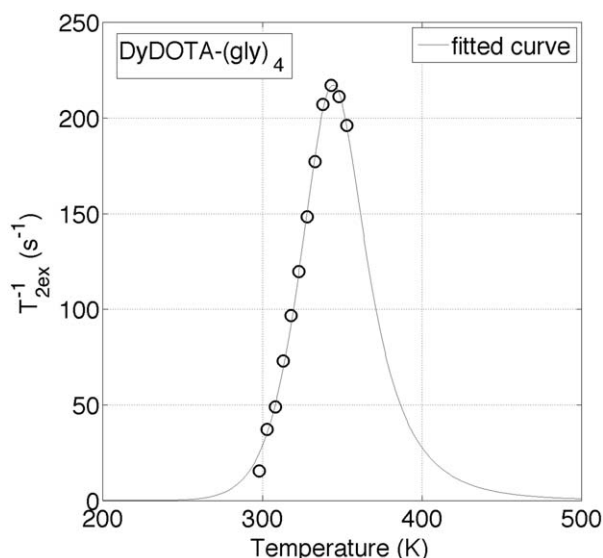


FIG. 3. A plot of the  $^{17}\text{O}$  measured exchange transverse relaxation rate ( $T_{2\text{ex}}^{-1}$ ) versus temperature for the  $\text{DyDOTA}(\text{gly})_4$  chelate. The least squares fit to the data (line) allows the water molecule exchange rate at 37°C to be calculated (39).

$$\tau_M^{-1} = \frac{k_{\text{ex}}^{298} T}{298.15} \exp \left[ \frac{\Delta H^\ddagger}{R} \left( \frac{1}{298.15} - \frac{1}{T} \right) \right] \quad [1]$$

where  $k_{\text{ex}}^{298}$  is the water molecule exchange rate at 25°C,  $T$  is temperature in Kelvin,  $\Delta H^\ddagger$  is the enthalpy of activation, and  $R$  is the universal gas constant. Similar fits were performed for the other  $\text{DyDOTA}(\text{amide})_x$  chelates. A full description of the  $^{17}\text{O}$  methods and Matlab fit can be found in the Supplementary Material.

The data from Table 1 can be more easily interpreted using a Swift-Connick plot (17) for  $\text{Dy}^{3+}$  at 400 MHz (9.4T) as shown in Figure 4. Swift-Connick theory (21) predicts that the transverse relaxivity due to water molecule exchange ( $r_{2\text{ex}}$ ) is a function of the bound water molecule lifetime ( $\tau_M$ ) as given by:

$$r_{2\text{ex}} = (1.8 \times 10^{-5}) \frac{\tau_M \Delta \omega^2}{1 + \tau_M^2 \Delta \omega^2} \quad [2]$$

where  $\Delta \omega$  is the paramagnetic frequency shift of the bound water molecule protons expressed in  $\text{rad s}^{-1}$  (17,40). Equation [2] predicts that for  $\text{Dy}^{3+}$  at 9.4T (using  $\Delta \omega = -730$  ppm or  $1.835 \times 10^6 \text{ rad s}^{-1}$ ) the  $r_{2\text{ex}}$  will

Table 1

Measured  $r_{2\text{tot}}$  and  $r_{2\text{ex}}$  Values for the Five  $\text{Dy}^{3+}$  Chelates Taken at Three Different Temperatures, Where  $r_{2\text{ex}} = r_{2\text{tot}} - r_{2\text{DyTETA}}$ <sup>a</sup>

$\text{Dy}^{3+}$ chelate	Total transverse relaxivity $r_{2\text{tot}}$ ( $\text{s}^{-1} \text{ mM}^{-1}$ )			Exchange transverse relaxivity $r_{2\text{ex}}$ ( $\text{s}^{-1} \text{ mM}^{-1}$ )			Bound water molecule lifetime $\tau_M$ (ns)		
	52°C	37°C	22°C	52°C	37°C	22°C	52°C	37°C	22°C
$\text{DyDOTA}$	0.17	0.43	1.5	0.01	0.22	1.3	0.8	3.7	22
$\text{DyDOTA}(\text{gly})_2$	3.7	9.9	18.8	3.6	9.7	18.6	93	190	400
$\text{DyDOTA}(\text{gly})_3$	13.2	12.0	4.2	13.0	11.8	3.9	330	1,800	7,700
$\text{DyDOTA}(\text{gly})_4$	8.6	3.6	1.4	8.5	3.4	1.2	1,800	4,900	14,000
$\text{DyTETA}$	0.16	0.21	0.22	(no water molecule exchange)					

<sup>a</sup>Also shown are the variable-temperature  $^{17}\text{O}$  measured bound water lifetimes. Compared to the other four chelates, the  $r_{2\text{tot}}$  for  $\text{DyTETA}$  is relatively independent of temperature due to the lack of water molecule exchange. Measurement errors for  $r_{2\text{tot}}$  and  $\tau_M$  were less than 10% and 20%, respectively.

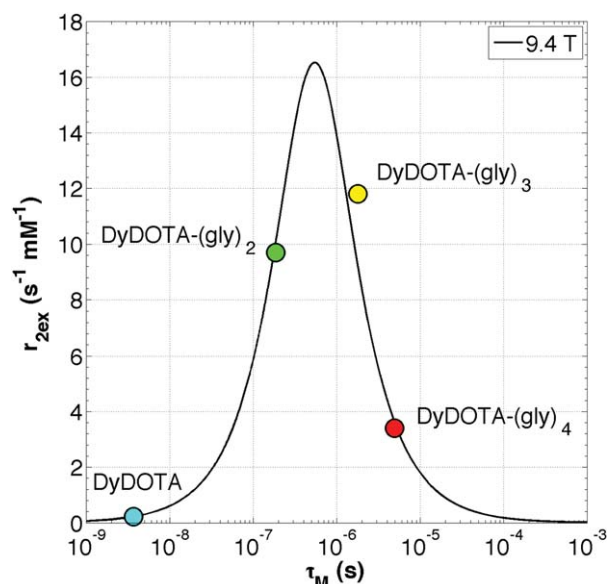
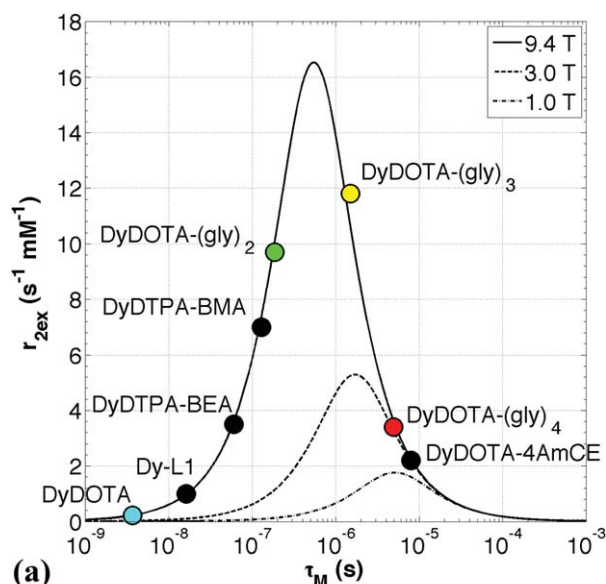


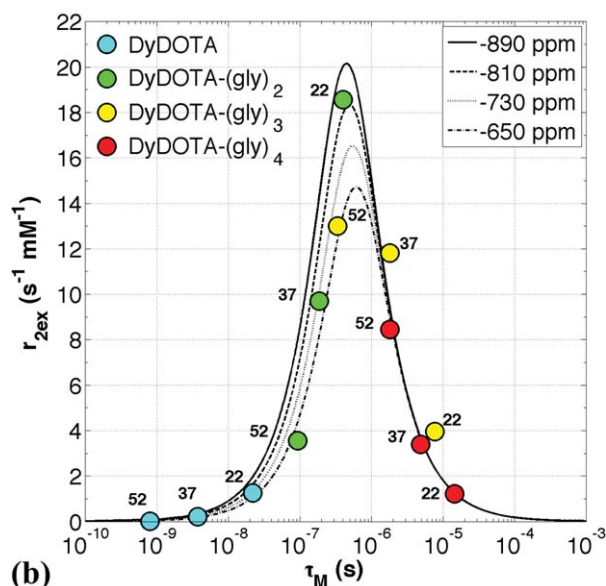
FIG. 4. A Swift-Connick plot for  $\text{Dy}^{3+}$  at 9.4T (400 MHz) using a  $\Delta\omega$  of  $-730$  ppm ( $1.835 \times 10^6$  rad  $\text{s}^{-1}$ ). Data markers for the measured  $r_{2\text{ex}}$  and  $\tau_M$  values at  $37^\circ\text{C}$  (from Table 1) are in excellent agreement with the Swift-Connick exchange theory, with DyDOTA-(gly)<sub>3</sub> giving the largest  $r_{2\text{ex}}$ .

reach a peak value of  $16.5 \text{ s}^{-1} \text{ mM}^{-1}$  at a specific bound water lifetime given by  $\Delta\omega^{-1} = 545$  ns. The “fast” side of the Swift-Connick plot is then defined as  $\tau_M < 545$  ns, while the “slow” side is defined as  $\tau_M > 545$  ns.

The  $37^\circ\text{C}$  data from Table 1 was plotted in Figure 4 for each DyDOTA-(amide)<sub>x</sub> chelate. It can be seen that the measured  $r_{2\text{ex}}$  and  $\tau_M$  data are in excellent agreement with the Swift-Connick theory. For example, while the faster water molecule exchange rate of DyDOTA places it on the fast side of the Swift-Connick peak, the slower water molecule exchange rate of DyDOTA-(gly)<sub>4</sub> places it on the slow side. This explains why  $r_{2\text{tot}}$  decreases with increasing temperature (smaller  $\tau_M$ ) for DyDOTA, yet increases with increasing temperature for DyDOTA-(gly)<sub>4</sub>. For DyDOTA-(gly)<sub>2</sub> and DyDOTA-(gly)<sub>3</sub>, their intermediate water molecule exchange rates place them



(a)



(b)

FIG. 6. a: A Swift-Connick plot comparing the new DyDOTA-(amide)<sub>x</sub> chelates (colored markers) to previous  $\text{Dy}^{3+}$ -based chelates (black markers) at 9.4T ( $\Delta\omega = -730$  ppm or  $1.835 \times 10^6$  rad  $\text{s}^{-1}$ ) and  $37^\circ\text{C}$ . Also shown is a Swift-Connick plot for  $\text{Dy}^{3+}$  at 3.0T ( $\Delta\omega = -730$  ppm or  $5.871 \times 10^5$  rad  $\text{s}^{-1}$ ). b: Swift-Connick plots for  $\text{Dy}^{3+}$  at 9.4T using four different values for  $\Delta\omega$ . Data markers for each chelate are shown (from Table 1) with temperatures given in  $^\circ\text{C}$ . Note that the abscissa and ordinate ranges are different in (a) and (b).

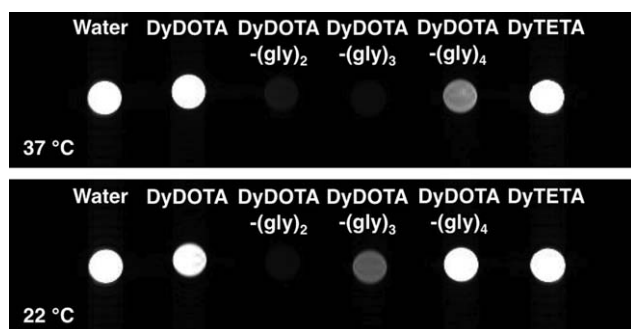


FIG. 5. Fast spin-echo images ( $TE = 12.4$  ms) of the five  $\text{Dy}^{3+}$  chelates (and water standard) in 5 mm diameter vials taken at 9.4T. By taking the same image at two different temperatures the dependence of  $T_{2\text{ex}}$  (and thus the total  $T_2$  contrast) upon the water molecule exchange rate can be qualitatively shown. The brightness and contrast levels for each image are the same.

close to the peak maximum in of the Swift-Connick plot. Figure 4 shows that at  $37^\circ\text{C}$  the highest  $r_{2\text{ex}}$  value is given by DyDOTA-(gly)<sub>3</sub> ( $11.8 \text{ s}^{-1} \text{ mM}^{-1}$  or 72% of the maximum  $r_{2\text{ex}}$ ) making it a potential candidate for development into a  $T_2$  contrast agent.

The effect that  $\tau_M$  has on  $T_{2\text{ex}}$ , and thus the total  $T_2$  contrast, can be qualitatively observed in the in vitro images shown in Figure 5. The top row shows a fast spin-echo image of a water standard and the five  $\text{Dy}^{3+}$  chelates (each at 20 mM) taken at  $37^\circ\text{C}$ . It can be seen that the signal intensities for DyDOTA (fast water molecule exchange) and DyTETA (no exchange) are similar to

that of pure water, indicating little or no  $T_2$  contrast at this TE value (12.4 ms). Yet for the remaining three chelates, their level of  $T_2$  contrast (i.e., darkening) is proportional to their vertical position ( $r_{2\text{ex}}$  value) on the Swift-Connick plot in Figure 4, with DyDOTA-(gly)<sub>3</sub> having the largest  $r_{2\text{ex}}$  value (11.8 s<sup>-1</sup> mM<sup>-1</sup>) and thus the darkest vial. The bottom row shows a similar fast spin-echo image but now at 22°C. The slower water molecule exchange at this temperature leads to different  $\tau_M$  and thus  $r_{2\text{ex}}$  values for each DyDOTA-(amide)<sub>x</sub> chelate, with DyDOTA-(gly)<sub>2</sub> now having the largest  $r_{2\text{ex}}$  value (18.6 s<sup>-1</sup> mM<sup>-1</sup>) and the darkest vial (see Fig. 6b). Similar in vitro spin-echo images for two DyDTPA-based chelates at 4.7T and 25°C was shown by Vander Elst et al (19) where one vial appears darker simply due to the difference in  $\tau_M$  and thus  $T_{2\text{ex}}$ .

## DISCUSSION

It is interesting to compare these new DyDOTA-(amide)<sub>x</sub> chelates to previous Dy<sup>3+</sup>-based  $T_2$  contrast agents that have reported  $\tau_M$  and  $r_2$  data. Figure 6a displays experimental data (black symbols) for DyDOTA-4AmCE (35), DyDTPA-BMA (39), DyDTPA-BEA (19), and Dy-L1 (the Dy<sup>3+</sup> analog of the Gd<sup>3+</sup>-based human serum albumin binding MS-325 blood pool agent) (20,41) on a Swift-Connick plot for 9.4T ( $\Delta\omega = -730$  ppm). The  $\tau_M$  values at 37°C (calculated from <sup>17</sup>O data and Eq. [1] when not directly given) were 8  $\mu$ s, 128.2 ns, 60 ns, and 16.1 ns, respectively. These  $\tau_M$  values were then used to estimate the  $r_{2\text{ex}}$  values at 9.4T by means of Figure 6a, which gave 2.2, 7.0, 3.5, and 1.0 s<sup>-1</sup> mM<sup>-1</sup>, respectively. These estimated  $r_{2\text{ex}}$  values are in agreement with their previously reported  $r_2$  data at 9.4T. It can be seen that these previous Dy<sup>3+</sup> chelates all had water molecule exchange rates that were either too fast or too slow to maximize  $r_{2\text{ex}}$  at 9.4T. Although DyDTPA-BMA gives an  $r_{2\text{ex}}$  value of approximately 7 s<sup>-1</sup> mM<sup>-1</sup>, it is still less than half of the maximum (16.5 s<sup>-1</sup> mM<sup>-1</sup>). Due to their intermediate water molecule exchange rates at 37°C, both DyDOTA-(gly)<sub>2</sub> and DyDOTA-(gly)<sub>3</sub> give higher  $r_{2\text{ex}}$  values at 9.4T. Although the  $\tau_M$  values for these two chelates are not quite at the ideal time of 545 ns, their  $r_{2\text{ex}}$  values are 59% and 72% the maximum respectively. These relative differences in  $r_{2\text{ex}}$  values become even more pronounced at fields lower than 9.4T, where the maximum  $r_{2\text{ex}}$  value reduces proportionately and moves toward slower exchange (larger  $\tau_M$ ) as shown in the 3.0T plot in Figure 6a. For example, at 9.4T (and 37°C) there is a 41% drop in  $r_{2\text{ex}}$  when moving from DyDOTA-(gly)<sub>3</sub> to DyDTPA-BMA (11.8 to 7.0 s<sup>-1</sup> mM<sup>-1</sup>), yet at 3.0T this reduction is 85% (5.3 to 0.8 s<sup>-1</sup> mM<sup>-1</sup>). Also, at 3.0T the peak  $r_{2\text{ex}}$  value of 5.3 s<sup>-1</sup> mM<sup>-1</sup> occurs at  $\Delta\omega^{-1} = (5.871 \times 10^5 \text{ rad s}^{-1})^{-1} = 1703$  ns, which makes the DyDOTA-(gly)<sub>3</sub> chelate ( $\tau_M = 1795$  ns at 37°C) ideally suited for use at 3.0T.

In Figure 4, it was assumed that all of the DyDOTA-(amide)<sub>x</sub> chelates studied here shared the same <sup>1</sup>H  $\Delta\omega$  value of -730 ppm (11). Yet there is evidence from the  $r_{2\text{ex}}$  and  $\tau_M$  data that the  $\Delta\omega$  values do vary slightly between chelates. This should be expected because of their different chemical structures and ligand fields surrounding the Dy<sup>3+</sup> ion. Figure 6b shows a Swift-Connick plot for Dy<sup>3+</sup> at 9.4T (400 MHz) where four different val-

ues for  $\Delta\omega$  have been plotted (see Eq. [2]). It can be seen that as the absolute value of  $\Delta\omega$  increases, the maximum  $r_{2\text{ex}}$  value increases proportionally and moves toward faster exchange. It can also be seen that while there is little difference between the Swift-Connick plots on the slow side, where the four curves converge, there is a significant difference on the fast side and most notably in the peak maximum. By using the  $r_{2\text{ex}}$  data for all three temperatures measured in Table 1 and their corresponding calculated  $\tau_M$  values, one can see how the  $r_{2\text{ex}}$  for each chelate varies with  $\tau_M$  in Figure 6b. All of these data appear to be in fairly good agreement with  $\Delta\omega = -730$  ppm except for DyDOTA-(gly)<sub>2</sub> at 22°C (green circle at  $\tau_M = 400$  ns) which, due to its high  $r_{2\text{ex}}$  value of 18.6 s<sup>-1</sup> mM<sup>-1</sup>, appears to agree with a larger  $\Delta\omega$  of around -810 ppm. Yet for DyDOTA-(gly)<sub>3</sub> at 52°C (yellow circle at  $\tau_M = 330$  ns) the experimental  $r_{2\text{ex}}$  value of 13.0 s<sup>-1</sup> mM<sup>-1</sup> is more consistent with a lower  $\Delta\omega$  of around -650 ppm, even though it shares a similar  $\tau_M$ . This could be explained by the two chelates having different chemical fields that lead to different  $\Delta\omega$  values and also by the variation of  $\Delta\omega$  with temperature, where the absolute value of  $\Delta\omega$  is inversely proportional to temperature. It is well known that hyperfine shifts such as these are extremely sensitive to temperature (42) so the exact shape and magnitude of these Swift-Connick type plots may depend upon getting a precise determination of  $\Delta\omega$  from hyperfine shift measurements of other nonexchanging protons in these paramagnetic complexes by high resolution NMR spectroscopy. These observations agree with quantitative estimates of the bound water molecule <sup>1</sup>H  $\Delta\omega$  made by measuring the chemical shifts of the cyclen H<sub>4</sub> protons in the DOTA ligand as a function of temperature (see Supplementary Material) (11).

## CONCLUSIONS

These data represent the first time that  $T_{2\text{ex}}$  for a series of DyDOTA-(amide)<sub>x</sub> chelates has been optimized by methodically adjusting the inner-sphere water molecule exchange rate at 9.4T and 37°C. To achieve the goal of having an  $r_{2\text{ex}}$  value greater than 10 s<sup>-1</sup> mM<sup>-1</sup>, the  $\tau_M$  needed to be in the "Goldilocks Zone" (43) (i.e., not too fast, not too slow, but just right) of approximately 200 ns to 2000 ns, with DyDOTA-(gly)<sub>3</sub> meeting this requirement ( $\tau_M = 1800$  ns,  $r_{2\text{ex}} = 11.8$  s<sup>-1</sup> mM<sup>-1</sup>) and DyDOTA-(gly)<sub>2</sub> coming close ( $\tau_M = 190$  ns,  $r_{2\text{ex}} = 9.7$  s<sup>-1</sup> mM<sup>-1</sup>). Preliminary in vivo results from the DyDOTA-(gly)<sub>2</sub> chelate showed a promising order of magnitude improvement in dose sensitivity compared with the EuDOTA-(gly)<sub>4</sub> chelate (44). Polymerization or dendrimerization of these chelates could further increase the  $r_{2\text{ex}}$  (per molecule) by a factor of 100 to approximately 1000 to 1200 s<sup>-1</sup> mM<sup>-1</sup> thereby creating highly sensitive, molecule-sized  $T_2$  contrast agents for MRI. These data also stress the importance of selecting the correct water molecule exchange rate (and  $\Delta\omega$ ) when designing lanthanide-based contrast agents as recently described by Sherry and Wu (45).

## ACKNOWLEDGMENTS

The authors thank Dr. Yunkou Wu for his guidance with these experiments, and also acknowledge Dr. R.H.E.



Hudson and the University of Western Ontario ASPIRE award for supporting Mark Milne's visit to the Advanced Imaging Research Center at UT Southwestern.

## REFERENCES

- Lauterbur PC. Image formation by induced local interactions - examples employing nuclear magnetic-resonance. *Nature* 1973;242:190-191.
- Damadian R, Goldsmith M, Minkoff L. NMR in cancer: XVI. FONAR image of live human body. *Physiol Chem Phys M* 1977;9:97-100.
- Damadian R. Tumor detection by nuclear magnetic resonance. *Science* 1971;171:1151-1153.
- Lauffer RB. Paramagnetic metal-complexes as water proton relaxation agents for NMR imaging - theory and design. *Chem Rev* 1987;87:901-927.
- Caravan P, Ellison JJ, McMurry TJ, Lauffer RB. Gadolinium(III) chelates as MRI contrast agents: structure, dynamics, and applications. *Chem Rev* 1999;99:2293-2352.
- Yoo B, Pagel MD. An overview of responsive MRI contrast agents for molecular imaging. *Front Biosci* 2008;13:1733-1752.
- Viswanathan S, Kovacs Z, Green KN, Ratnakar SJ, Sherry AD. Alternatives to gadolinium-based metal chelates for magnetic resonance imaging. *Chem Rev* 2010;110:2960-3018.
- Solomon I. Relaxation processes in a system of 2 spins. *Phys Rev* 1955;99:559-565.
- Weissleder R, Elizondo G, Wittenberg J, Rabito CA, Bengel HH, Josephson L. Ultrasmall superparamagnetic iron-oxide - characterization of a new class of contrast agents for MR imaging. *Radiology* 1990;175:489-493.
- Opina ACL, Ghaghada KB, Zhao PY, Kiefer G, Annapragada A, Sherry AD. TmDOTA-tetraglycinate encapsulated liposomes as pH-sensitive LipoCEST agents. *Plos One* 2011;6:e27370.
- Zhang SR, Sherry AD. Physical characteristics of lanthanide complexes that act as magnetization transfer (MT) contrast agents. *J Solid State Chem* 2003;171:38-43.
- Aime S, Barge A, Castelli DD, Fedeli F, Mortillaro A, Nielsen FU, Terreno E. Paramagnetic lanthanide(III) complexes as pH-sensitive chemical exchange saturation transfer (CEST) contrast agents for MRI applications. *Magn Reson Med* 2002;47:639-648.
- Ward KM, Aletras AH, Balaban RS. A new class of contrast agents for MRI based on proton chemical exchange dependent saturation transfer (CEST). *J Magn Reson* 2000;143:79-87.
- Vinogradov E, Sherry AD, Lenkinski RE. CEST: from basic principles to applications, challenges and opportunities. *J Magn Reson* 2013; 229:155-172.
- Hancu I, Dixon WT, Woods M, Vinogradov E, Sherry AD, Lenkinski RE. CEST and PARACEST MR contrast agents. *Acta Radiol* 2010;51: 910-923.
- Zhang S, Winter P, Wu K, Sherry AD. A novel europium(III)-based MRI contrast agent. *J Am Chem Soc* 2001;123:1517-1518.
- Soesbe TC, Merritt ME, Green KN, Rojas-Quijano FA, Sherry AD. T(2) Exchange agents: a new class of paramagnetic MRI contrast agent that shortens water T(2) by chemical exchange rather than relaxation. *Magn Reson Med* 2011;66:1697-1703.
- Pintacuda G, John M, Su XC, Otting G. NMR structure determination of protein-ligand complexes by lanthanide labeling. *Acc Chem Res* 2007;40:206-212.
- Vander Elst L, Roch A, Gillis P, Laurent S, Botteman F, Bulte JWM, Muller RN. Dy-DTPA derivatives as relaxation agents for very high field MRI: the beneficial effect of slow water exchange on the transverse relaxivities. *Magn Reson Med* 2002;47:1121-1130.
- Caravan P, Greenfield MT, Bulte JWM. Molecular factors that determine Curie spin relaxation in dysprosium complexes. *Magn Reson Med* 2001;46:917-922.
- Swift TJ, Connick RE. NMR-relaxation mechanisms of O17 in aqueous solutions of paramagnetic cations and the lifetime of water molecules in the first coordination sphere. *J Chem Phys* 1962;37:307-321.
- Rabenstein DL, Fan S. Proton nuclear-magnetic-resonance spectroscopy of aqueous-solutions - complete elimination of the water resonance by spin spin relaxation. *Anal Chem* 1986;58:3178-3184.
- Aime S, Nano R, Grandi M. A new class of contrast agents for magnetic-resonance imaging based on selective reduction of water-T2 by chemical-exchange. *Invest Radiol* 1988;23:S267-S270.
- Aime S, Calabi L, Biondi L, De Miranda M, Ghelli S, Paleari L, Rebaudengo C, Terreno E. Iopamidol: exploring the potential use of a well-established X-ray contrast agent for MRI. *Magn Reson Med* 2005; 53:830-834.
- Aime S, Botta M, Barbero L, Uggeri F, Fedeli F. Water signal suppression by T2-relaxation enhancement promoted by Dy(III) complexes. *Magn Reson Chem* 1991;29:S85-S88.
- Saeed M, Wendland MF, Tomei E, Rocklage SM, Quay SC, Moseley ME, Wolfe C, Higgins CB. Demarcation of myocardial ischemia - magnetic-susceptibility effect of contrast-medium in MR imaging. *Radiology* 1989;173:763-767.
- Nilsson S, Wikstrom G, Ericsson A, Wikstrom M, Oksendal A, Waldenstrom A, Hemmingsson A. Myocardial cell death in reper-fused and nonreperused myocardial infarctions - MR imaging with dysprosium-DTPA-BMA in the pig. *Acta Radiol* 1996;37:18-26.
- Nilsson S, Wikstrom G, Ericsson A, Wikstrom M, Oksendal A, Waldenstrom A, Hemmingsson A. Double-contrast mr imaging of reperused porcine myocardial infarction - an experimental study using Gd-DTPA-BMA and Dy-DTPA-BMA. *Acta Radiol* 1996;37:27-35.
- Saeed M, Wendland MF, Masui T, Higgins CB. Reperused myocardial infarctions on T1- and susceptibility-enhanced MRI - evidence for loss of compartmentalization of contrast-media. *Magn Reson Med* 1994;31:31-39.
- Zhao SH, Revel D, Arteaga C, Canet E, Liu SZ, Hadour G, Forrat R, Oksendal A. Magnetic susceptibility of Dy-DTPA-BMA to reperused myocardial infarction in an excised dog heart model: evidence of viable myocardium. *Chin Med J* 2000;113:260-264.
- Wang C, Sundin A, Ericsson A, BachGansmo T, Hemmingsson A, Ahlstrom H. Dysprosium-enhanced MR imaging for tumor tissue characterization - An experimental study in a human xenograft model. *Acta Radiol* 1997;38:281-286.
- Roberts TPL, Kucharczyk J, Cox I, Moseley ME, Prayer L, Dillon W, Bleyl K, Harnish P. Sprodiamide-injection-enhanced magnetic resonance imaging of cerebral perfusion. Phase I clinical-trial results. *Invest Radiol* 1994;29:S24-S26.
- Bulte JWM, Wu CC, Brechbiel MW, Brooks RA, Vymazal J, Holla M, Frank JA. Dysprosium-DOTA-PAMAM dendrimers as macromolecular T2 contrast agents - preparation and relaxometry. *Invest Radiol* 1998;33:841-845.
- Fossheim SL, Kellar KE, Mansson S, Colet JM, Rongved P, Fahlvik AK, Klaveness J. Investigation of lanthanide-based starch particles as a model system for liver contrast agents. *J Magn Reson Imaging* 1999; 9:295-303.
- Vander Elst L, Zhang S, Sherry AD, Laurent S, Botteman F, Muller RN. Dy-complexes as high field T2 contrast agents: influence of water exchange rates. *Acad Radiol* 2002;9:S297-S299.
- Desreux JF. Nuclear magnetic-resonance spectroscopy of lanthanide complexes with a tetraacetic tetraaza macrocycle - unusual conformation properties. *Inorg Chem* 1980;19:1319-1324.
- Kovacs Z, Sherry AD. A general-synthesis of 1,7-Disubstituted 1,4,7,10-tetraazacyclododecanes. *J Chem Soc Chem Comm* 1995:185-186.
- Green KN, Viswanathan S, Rojas-Quijano FA, Kovacs Z, Sherry AD. Europium(III) DOTA-derivatives having ketone donor pendant arms display dramatically slower water exchange. *Inorg Chem* 2011;50: 1648-1655.
- Pubanz D, Gonzalez G, Powell DH, Merbach AE. Unexpectedly large change of water exchange-rate and mechanism on [Ln(Dtpa-Bma)(H2O)] complexes along the Lanthanide(III) series. *Inorg Chem* 1995;34:4447-4453.
- Granot J, Fiat D. Effect of chemical exchange on transverse relaxation rate of nuclei in solution containing paramagnetic-ions. *J Magn Reson* 1974;15:540-548.
- Lauffer RB, Parmelee DJ, Dunham SU, Ouellet HS, Dolan RP, Witte S, McMurry TJ, Walovitch RC. MS-325: albumin-targeted contrast agent for MR angiography. *Radiology* 1998;207:529-538.
- Peters JA, Huskens J, Raber DJ. Lanthanide induced shifts and relaxation rate enhancements. *Prog Nucl Magn Reson Spectrosc* 1996;28: 283-350.
- Seager S. Exoplanet habitability. *Science* 2013;340:577-581.
- Soesbe TC, Ratnakar JS, Kovacs Z, Sherry AD. Using T2-exchange from Dy3+DOTA-based chelates for contrast-enhanced molecular imaging with MRI. In Proceedings of the 21st Annual Meeting of ISMRM, Salt Lake City, Utah, USA, 2013. Abstract 1909.
- Sherry AD, Wu YK. The importance of water exchange rates in the design of responsive agents for MRI. *Curr Opin Chem Biol* 2013;17: 167-174.

## Advancing the early detection and diagnosis of primary and recurring thyroid cancers using a molecularly targeted T<sub>2</sub>-exchange MRI contrast agent

Todd C. Soesbe<sup>1,2\*</sup>, S. James Ratnakar<sup>1</sup>, Mark Milne<sup>1</sup>, Fiemu Nwariaku<sup>3</sup>, A. Dean Sherry<sup>1,4</sup>, and Robert E. Lenkinski<sup>2,1</sup>

<sup>1</sup>Advanced Imaging Research Center, UT Southwestern Medical Center, Dallas, Texas. <sup>2</sup>Department of Radiology, UT Southwestern Medical Center, Dallas, Texas. <sup>3</sup>Department of Surgery, UT Southwestern Medical Center, Dallas, Texas. <sup>4</sup>Department of Chemistry, University of Texas, Dallas, Texas.

**Target audience:** This will benefit Scientists and Physicians interested in the chemical engineering, development, and pre-clinical *in vivo* imaging of molecularly targeted T<sub>2</sub> MRI contrast agents for the early detection and diagnosis of cancer.

**Purpose:** The early detection and diagnosis of both primary and recurring cancerous lesions is essential to the successful treatment of aggressive thyroid cancer. Ultrasound imaging offers high-resolution and easy acquisition, but it lacks functional information, tissue specificity, and whole-body field of view capabilities. SPECT and PET offer very sensitive whole-body functional imaging, but suffer from low-resolution, warm and cold lesion indeterminacy, and require CT for anatomic correlation. Furthermore, dual-modality SPECT/CT and PET/CT expose the subject to significant doses of ionizing radiation, making them impractical for frequent therapeutic monitoring in patients. In contrast, MRI offers superior anatomic resolution and soft tissue contrast as compared to SPECT/CT and PET/CT, making it an excellent tool for cancer detection. The effectiveness of MRI in the functional and molecular imaging regime is currently limited due to the lack of highly sensitive molecularly targeted contrast agents. Creating such agents would greatly improve the use of MRI for the early detection and diagnosis of thyroid cancer. Our research goal is to use the newly described phenomena of T<sub>2</sub>-exchange (T<sub>2ex</sub>) to create highly sensitive, targeted, and molecule-sized T<sub>2</sub> contrast agents for enhanced molecular imaging of thyroid cancer with MRI.

**Methods:** Four different versions of the DyDOTA-(gly)<sub>x</sub> chelate (i.e., x=0,2,3,4) were synthesized, with each chelate having a different water molecule exchange rate ( $k_{ex}=\tau_M^{-1}$ ). The Dy<sup>3+</sup> ion was used because it has the largest bound water chemical shift and one of the largest paramagnetic relaxation enhancements of the Lanthanide metals (second only to Gd<sup>3+</sup>), both characteristics will maximize the level of T<sub>2</sub> contrast achieved for the monomer chelate ( $r_2 \sim 16 \text{ s}^{-1} \text{ mM}^{-1}$ ) as recently shown (1). The  $r_{2ex}$  and  $\tau_M$  values for each chelate were then experimentally measured at 37 °C using <sup>17</sup>O methods (1). As proof of principle to show the negative contrast capabilities of these new T<sub>2ex</sub> chelates, small doses were directly injected into mice brain and thyroid areas to simulate uptake due to molecular targeting. Animal data were acquired on an Agilent 9.4 T system.

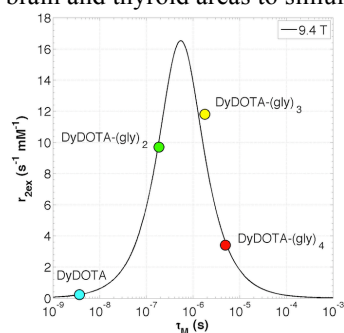


Fig. 1

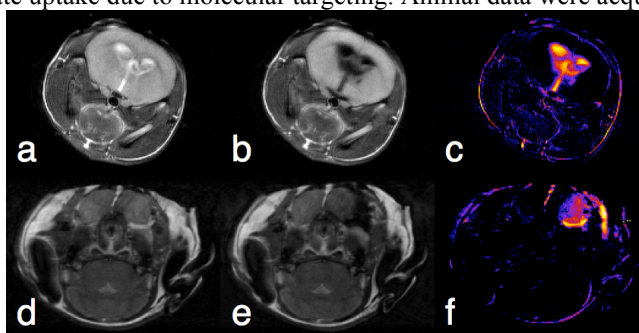


Fig. 2

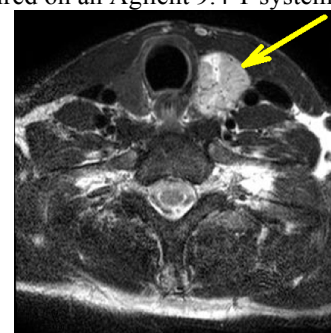


Fig. 3

**Results:** **Fig. 1:** A Swift-Connick plot showing the theoretical relation (black line) between the transverse relaxivity due to water molecule exchange ( $r_{2ex}$ ; y-axis) and the bound water lifetime ( $\tau_M$ ; x-axis) for Dy<sup>3+</sup> at 9.4 T. The ideal  $\tau_M$  is at 545 ns. The measured  $r_{2ex}$  and  $\tau_M$  values for the four different Dy<sup>3+</sup> chelates (colored markers) are in excellent agreement, with DyDOTA-(gly)<sub>2</sub> (green circle) and DyDOTA-(gly)<sub>3</sub> (yellow circle) giving the highest  $r_{2ex}$  values. **Fig. 2:** **a:** Axial MRI of a healthy mouse brain before intracranial injection of 30  $\mu\text{mol/kg}$  of DyDOTA-(gly)<sub>3</sub> in 20  $\mu\text{L}$  **b:** After intracranial injection. Note the darkening of ventricle CSF due to T<sub>2ex</sub>. **c:** The difference image a-b showing regions of agent uptake. **d:** Axial MRI of a healthy mouse thyroid before direct injection of 30  $\mu\text{mol/kg}$  of DyDOTA-(gly)<sub>3</sub> in 20  $\mu\text{L}$  **e:** After direct injection. Note the darkening of mouse's left thyroid/salivary gland area. **f:** The difference image d-e showing regions of agent uptake. **Fig. 3:** Axial MRI of a human thyroid nodule at 7.0 T. The nodule on patient's left (arrow), which appears bright under T<sub>2</sub> weighted MRI, would be an ideal target for a T<sub>2</sub> darkening contrast agent. Our goal is to target the cancerous regions of such nodules and lesions and make them "light up" as demonstrated in Fig. 2f. **Discussion:** We have previously shown that the Ln<sup>3+</sup>DOTA-based chelates (Ln<sup>3+</sup>≠La, Gd, Lu) create enhanced T<sub>2</sub> contrast (i.e., darkening) in MRI through the chemical exchange of water molecules (2). The level of this "T<sub>2</sub>-exchange" contrast is proportional to the bound water molecule chemical shift and reaches a maximum at a specific water molecule exchange rate. We have also previously demonstrated that T<sub>2ex</sub> contrast can be increased by several orders of magnitude through simple linear polymerization of the Ln<sup>3+</sup>DOTA chelate (3). We hypothesize that by using these two methods, a highly sensitive MRI T<sub>2</sub> contrast agent can be created while retaining the advantages of using small molecules rather than nanoparticles (e.g., SPIO) for improved biological targeting, uptake, and clearing. **Conclusion:** These T<sub>2ex</sub> contrast agents have the potential to accurately image the location and size of cancerous thyroid lesions and (by using receptors as prognostic indicators) differentiate between indolent and aggressive forms, thereby performing disease staging entirely non-invasively (i.e., without FNA biopsy). Also, in contrast to SPECT/CT or PET/CT, disease diagnostics and therapy monitoring would be performed on a single-modality MRI instrument without the risk of ionizing radiation. This would reduce patient stress by eliminating unnecessary thyroid resections and finding recurrence earlier. This technique could also be combined with spectroscopy of the choline peak to increase specificity (4).

**References:** (1) Soesbe TC, et al. MRM 2014;71:1179-1185. (2) Soesbe TC, et al. MRM 2011;66:1697-1703. (3) Wu Y, Soesbe TC, et al., JACS 2008;130:13854-13855. (4) Mountford C, et al. JMIR 2006;24:459-477.